

# Ammonia Bunker Vessel: Ship Design for Energy Transition

Friederike Dahlke-Wallat<sup>1</sup>, Katja Hoyer<sup>1</sup>, Ljubisav Isidorović<sup>1</sup>, Sophie Martens<sup>1</sup>, Nathalie Reinach<sup>1</sup>, Benjamin Friedhoff<sup>1</sup>, and Igor Bačkalov<sup>1,\*</sup>

## ABSTRACT

*This paper presents the basic design of a coastal ammonia carrier, intended to facilitate the energy transition by providing small-scale bunkering services to ferries in the South Baltic Sea. Due to the size and the purpose of the ship, a classic design process which builds on the experience and benefits from the prototype ships cannot be implemented in a straightforward manner. It follows that the energy transition may have a substantial impact on the design of otherwise conventional ship types, and that a hybrid approach to ship design comprising traditional design methodologies, advanced CAD tools, and experimentation is needed.*

## KEY WORDS

Ammonia; Energy transition; Bunker vessel; Coastal ship; CAMPFIRE.

## INTRODUCTION

Alternative fuels play a major role in the energy transition of shipping, whereby one of the considered solutions is ammonia. While most of the ship design studies focus on the development of ships powered by novel fuels, this paper addresses the development of the infrastructure necessary for the reliable supply of such fuels, which also includes new bunker ships. Namely, the technologies for both the waterborne transport of liquid ammonia and the (ship-to-ship and truck-to-ship) refueling of ships with ammonia are being developed. This paper presents the design of a coastal ammonia bunker vessel, which is intended to provide small-scale bunkering services to future ammonia-powered ferries operating in the South Baltic Sea.

Liquefied gas carriers have been in use since the 1930s. The current fleet stands at approximately 1600 units (see SIGTTO, 2021), whereby some 200 ships can carry ammonia as cargo (see DNV, 2020). Thus, it may be concluded that substantial experience in design of ammonia carriers already exists. Such experience, however, may be of limited assistance in the present study, as the coastal ammonia bunker vessel has several unique features setting it apart from the conventional gas carriers. To compensate for the absence of an appropriate prototype ship, the design process described in the paper utilizes a “hybrid” approach, where the traditional ship design methodology (characteristic for the “design spiral”) is blended with the advanced CAD tools, and the decision-making is supported by the statistical data on similar vessels, collected for the purpose of the study. Additional insights gained from the model tests are used primarily for the design appraisal but may also serve to assess the reliability of some of the classical methods for evaluation of powering requirements often used in early stages of design. Therefore, the purpose of the paper is two-fold. On the one hand, it explores the impact of energy transition on the design of bunker ships. On the other hand, it investigates the applicability of the classical methods in a design process which is handicapped by the lack of reliable data and by virtual nonexistence of the specific design guidelines.

---

<sup>1</sup> Development Centre for Ship Technology and Transport Systems (DST e. V.), Duisburg, Germany; ORCID: 0000-0002-1571-1361 (Friederike Dahlke-Wallat), 0000-0002-7366-1585 (Katja Hoyer), 0009-0001-1042-7134 (Nathalie Reinach), 0000-0002-5924-3563 (Benjamin Friedhoff), 0000-0002-6616-5516 (Igor Bačkalov)

\* Corresponding Author: [backalov@dst-org.de](mailto:backalov@dst-org.de)

## OWNER'S REQUIREMENTS AND DESIGN OBJECTIVES

The “owner’s requirements” follow from a scenario considered within the project. In future, the ammonia which can be supplied as fuel may be available from the tank storage in Peez situated in the vicinity of the port of Rostock. Alternatively, green ammonia may be collected from the offshore wind parks in the Baltic Sea. The ferries operating in the Baltic Sea have been identified as potential clients. Using Rostock as the homeport, the ship would supply with ammonia the long-range ferry sailing on the route Travemünde–Trelleborg and the short-range ferry sailing on the route Gedser–Rostock, see **Figure 1**. This determines the South Baltic Sea as the operational area of the ship. The principal “owner’s requirement” – cargo capacity of the ship – is decided based on the estimated requirements for ammonia as fuel of the two ferries: 650 m<sup>3</sup> and 300 m<sup>3</sup> of ammonia would be necessary for the long- and the short-range ferries respectively to complete their round trips. It follows that the ship’s cargo capacity should be around 1000 m<sup>3</sup>.

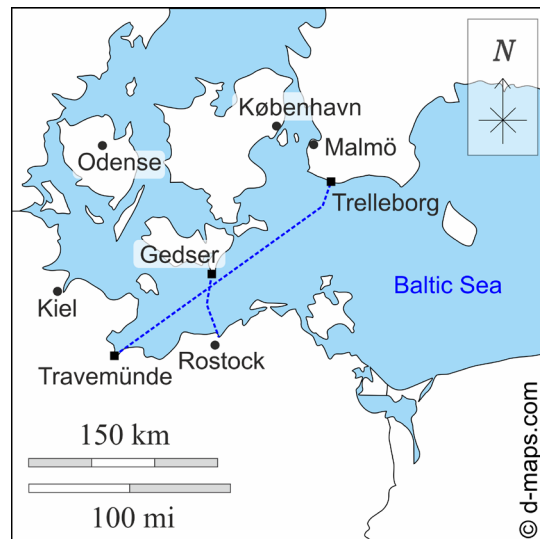


**Figure 1. Routes of (future) ammonia-powered ferries (base map: <https://d-maps.com/>).**

The targeted ship speed is 11 kn. The ship is to be conventionally powered to overcome the initial “supply-demand” obstacle of the green transition, that is, the limited implementation of greening technologies due to the lack of infrastructure providing sustainable alternative fuels which is, in turn, justified by the limited number of potential customers. An ammonia bunker vessel powered by diesel and/or drop-in fuels would be, therefore, an initial step towards the acceleration of the shipping energy transition.

Design objectives follow from the owner’s requirements. As with any cargo ship, the primary goal is to provide efficient transport and supply of the required cargo volume to the customers. The costs of the cargo tanks’ production should be low and cargo space should be easy to maintain. Thus, the geometry and arrangement of cargo tanks – which have to comply with the safety regulations – have a decisive influence on the design as a whole. The design should facilitate the bunkering operations and safe handling of ammonia, which also affects the design of the cargo tanks as well as the deck arrangement and positioning of the related equipment. Considering that the cargo capacity is relatively small, the ship will be small as well, which is not favorable from the seakeeping point of view. The seakeeping performance of the vessel may be improved to an extent with a favorable hull form (or its operation may be limited with respect to the relevant seakeeping criteria).

## SELECTION OF MAIN PARTICULARS

The ship design process usually benefits from a prototype vessel; if an adequate prototype is available, main dimensions may be selected with more confidence, weight estimation may be carried out with more precision, a range of technical solutions implemented on the prototype may be adopted, while the layout of the systems and the general arrangement of the prototype could be used as blueprints for the new design, and so on. It will be shown, however, that a suitable prototype is nonexistent in this case.

The initial selection of the main particulars (mass of displacement, length, beam, draught, depth, and hull form coefficients) was performed using the empiric regression formulae available from the literature (see Barras, 2006; Papanikolaou, 2014; Schneekluth and Bertram, 1998; Takahashi et al., 2006; Watson, 1998). However, it may be questioned how adequate such

formulae are considering that most of the authors used other ship types (such as e.g., general cargo ships and bulk carriers) in generating the underlying databases, with only occasional references to ship types which are only marginally relevant for this study, such as oil tankers. Additionally, it should be taken into account that some formulae were based on nowadays outdated hull forms and ship types, as pointed out by Papanikolaou (2014). Therefore, to verify the fitness of thus obtained values, a database containing the information on 41 relevant ships (liquefied gas carriers, chemical tankers, product carriers, bunker vessels, etc.) was created for the purpose of this study using a range of sources (hereinafter “DST database”). The features of the database are reported in the Appendix to this paper.

Assuming that the mass of deadweight is approximately:

$$m_{DWT} \approx 1.1 \cdot m_{cargo} \quad [1]$$

the first estimation of the mass of ship displacement may be done using the deadweight coefficient, expressed as the deadweight-over-displacement ratio:

$$\eta_{DWT} = \frac{m_{DWT}}{\Delta} \quad [2]$$

The deadweight coefficient may significantly vary depending on the ship type, so its value should be carefully selected. In the examined case, however, this is not a trivial task, because the references to adequate ship types (e.g., liquefied gas carriers) are seldom. In addition, a difference in density of liquefied ammonia ( $\rho_{NH_3} = 0.68 \text{ t/m}^3$ ) when compared to LPG ( $\rho_{LPG} = 0.525\text{--}0.58 \text{ t/m}^3$ ) and LNG ( $\rho_{LNG} = 0.43\text{--}0.48 \text{ t/m}^3$ ) exemplifies the uncertainty related to a proper selection of the deadweight coefficient. Barras (2004) reports  $\eta_{DWT} = 0.62$  for “LNG or LPG ships”. Takahashi et al. (2006), on the other hand, report  $\eta_{DWT} = 0.72$  for LNG ships. In addition to the difference in cargo density, this value is found not to be relevant for the present study, as it was obtained by analyzing mostly very large ships: gross tonnage of more than 90% of the analyzed LNG ships was greater than 30000 GT, while small ships made less than 2% of the database used by Takahashi et al. (2006). On the other hand, the LPG carriers analyzed by Takahashi et al. (2006) feature two distinct groups of vessels: ships up to 50000 GT and ships around 100000 GT. Considering that only the smaller ships are of interest for the present study, a displacement-gross tonnage relation applicable to ships up to 50000 GT was established. Based on this  $\Delta$ –GT relation and the available  $m_{DWT}$ –GT relation, it follows that the deadweight coefficient of LPG carriers (of up to 50000 GT) would be  $\eta_{DWT} = 0.625$ . Finally, the DST database of relevant ships shows that there is a strong correlation between the displacement of the ships and their cargo capacity (coefficient of determination of the regression line is  $R^2 = 0.955$ ), see **Figure 2**, which can be expressed as:

$$\Delta = 1.6374 \cdot V_{cargo} - 219.73 . \quad [3]$$

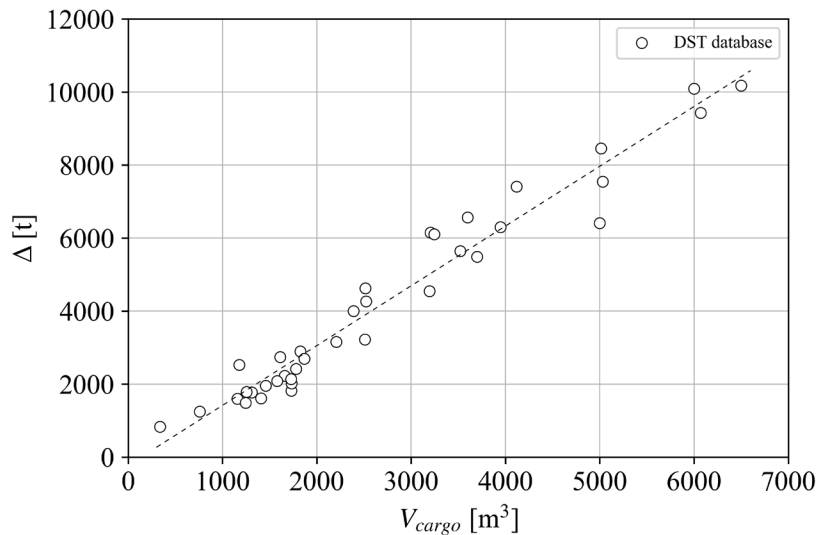


**Figure 2. Correlation of ship displacement and volume of the cargo tanks of the relevant ships in the DST database.**

The preliminary estimation of displacement is thus adopted as the average of the three values which are computed based on Barras (2004), Takahashi et al. (2006) for ships of up to 50000 GT, and equation [3]. This allows for assessment of the ship

length  $L$  which is computed as the average of five values ranging from 55.7 m to 60.8 m, obtained by regression formulae given in Papanikolaou (2014), Takahashi et al. (2006), and Watson (1998). The ship beam  $B$  is estimated based on considerations of Takahashi et al. (2006), and Watson (1998). The block coefficient  $C_B$  is decided based on the range of recommendations (mostly related to the Froude number of the ship) given in Schneekluth and Bertram (1998) and Watson (1998). The longitudinal center of buoyancy  $LCB$  is estimated based on the recommendations given in Schneekluth and Bertram (1998) and Papanikolaou (2014). Once the values of  $\Delta$ ,  $L$ ,  $B$ , and  $C_B$  are known, calculating design draught  $d$  is straightforward. Nevertheless, each of the parameters could be subject to further refinement. In addition, even though the values of some of the parameters, such as the block coefficient, may be indicative of the existing designs if obtained by empiric formulae, they may as well be a matter of decision which deviates to an extent from the calculated values, depending on the targeted performance. A similar argument applies to the waterplane area coefficient  $C_{WL}$  which may be calculated using the empiric formulae as well (such as the ones provided by Papanikolaou, 2014) but may be also reconsidered in light of a specific design aspect. For instance, the  $C_{WL}$  value may be tuned aiming at improved seakeeping performance: to improve seaworthiness and diminish the resonance of heave and pitch in head seas, the non-dimensional natural heave and pitch periods should be as short as possible which may be achieved by the increase of the waterplane area coefficient (with unchanged values of the main dimensions, displacement, and speed). The midship area coefficient  $C_M$  is calculated as the average of three values obtained using formulae given in Schneekluth and Bertram (1998). The depth of ship  $D$ , as a minimum, should comply with the requirements of the International Convention on Load Lines (ICLL, 2003) for Type A ships. The first estimate of the main particulars is reported in **Table 1**.

**Table 1: First estimate of the main ship particulars**

Cargo capacity	$V_{cargo}$	1000 m <sup>3</sup>
Mass of deadweight	$m_{DWT}$	750 t
Displacement	$\Delta$	1275 t
Length	$L$	58 m
Beam	$B$	10.5 m
Draught	$d$	3.26 m
Depth	$D$	3.87 m
Freeboard	$f$	0.61 m
Block coefficient	$C_B$	0.626
Waterplane area coefficient	$C_{WL}$	0.790
Midship area coefficient	$C_M$	0.969
Longitudinal center of buoyancy	$LCB^*$	-2 % $L$

\* In reference to midships

The estimated main particulars were subsequently compared to the trends observed in the DST database of relevant ships (note that the trendlines shown in **Figure 3** are indicative only and were not used in the calculation of the main particulars). **Figure 3a** and **Figure 3b** show that the first estimates of length and beam fit well into the trends detected for the existing ships. This may not be stated for the estimated design draught, which appears to be lower than what could be expected for the ship of the given cargo capacity, see **Figure 3c**. As previously pointed out, the draught depends on the block coefficient, provided that  $L$ ,  $B$ , and  $\Delta$  are fixed. However, there is no clear trend in the  $C_B$  values of the existing ships, as may be seen in **Figure 3e**. The scatter of  $C_B$  values is particularly large for ships of smaller cargo capacity, up to 2500 m<sup>3</sup>. An increase of the draught would imply a further decrease of the (already relatively low) block coefficient, which could result in a loss of volume available for the cargo space, and, consequently, complex geometry and high production costs of cargo tanks. On the other hand, increase of the block coefficient would lead to a further decrease of the draught, which is generally favorable from the cargo stowage point of view but may lead to a higher frequency of slamming. Block coefficient is equally poorly correlated to the Froude number, see **Figure 3f**. The absence of correlation of  $C_B$  to both  $V_{cargo}$  and  $Fr$ , confirms that the block coefficient is often a matter of a deliberate choice rather than an outcome of a statistical analysis. Ship depth is also well correlated to cargo volume of the existing ships, see **Figure 3d**. A weaker correlation is found between the freeboard  $f$  and ship length, see **Figure 4**. A higher freeboard implies improved safety (greater righting lever, larger reserve buoyancy, and lower frequency of shipping of green water) but comes at a cost (e.g., increase of operational costs related to higher gross tonnage). The deviation of the freeboard of the existing ships from the minimum freeboard as prescribed by the International Convention on Load Lines (ICLL, see IMO, 2003) may be substantial and may vary considerably for the ships of approximately the same length. It follows that the selection of  $f$  and  $D$  is not straightforward and that it is probably guided by the suitability of space for cargo stowage. As a first estimate, the selected freeboard is close to the minimum value required by IMO (2003) since the trends observed for the existing ships of similar lengths comply well with the ICLL provisions.

Finally, it should be noted there are only two ships with  $V_{cargo} \leq 1000 \text{ m}^3$  in the DST database (i.e., less than 5% of the total number of ships in the database): a chemical tanker and a product tanker. This highlights the difficulty of finding an adequate prototype ship.

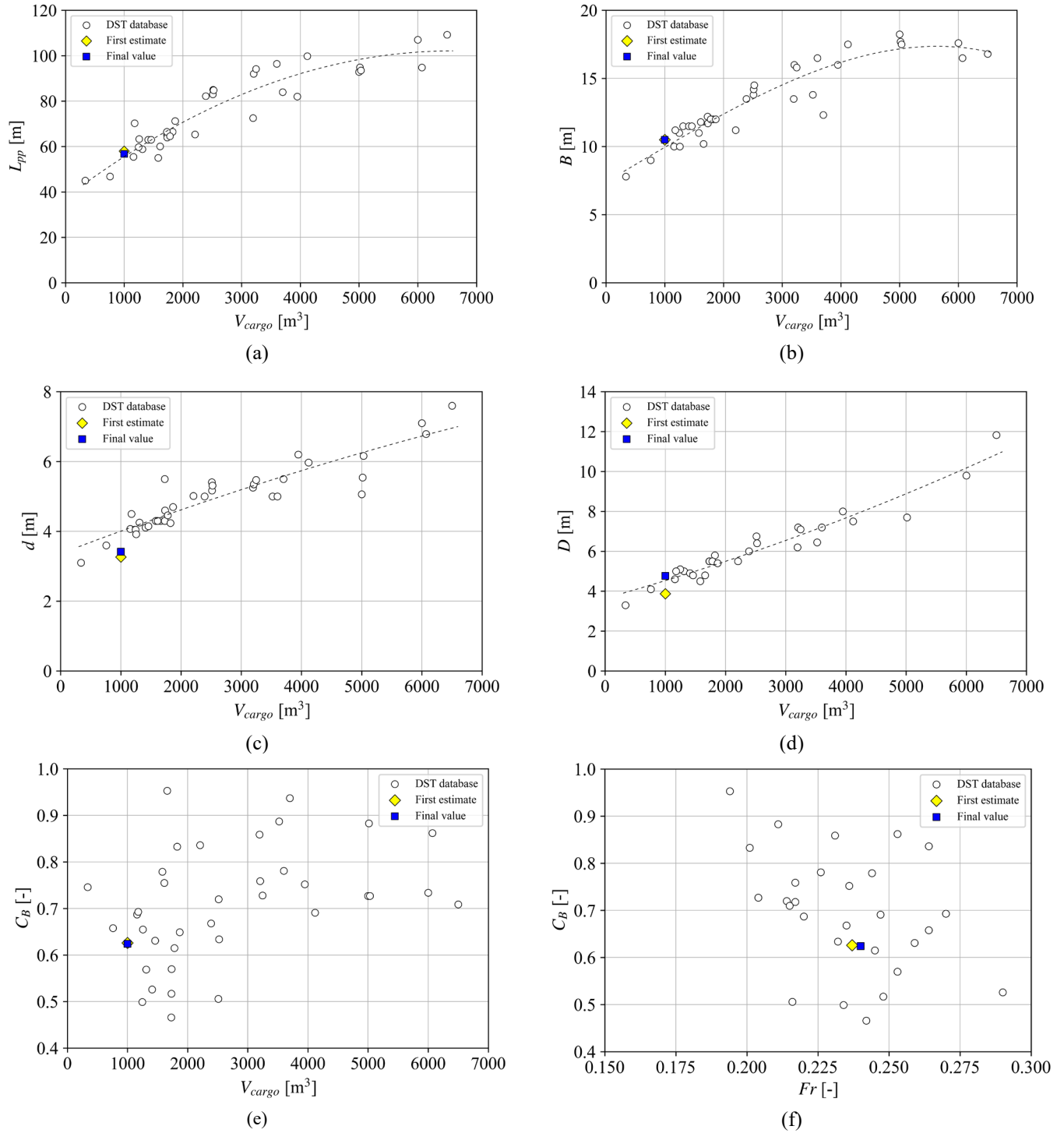


**Figure 3. Comparison of estimated and adopted ship particulars to the trends observed in the DST database of relevant ships. Yellow diamonds correspond to the first estimate of the ship particulars (reported in Table 1). Blue squares correspond to the final values of the ship particulars (reported in Table 2).**

Once the main particulars are selected, the preliminary stability assessment and resistance prediction may be performed, and the so-called “weight groups” may be estimated by means of approximate formulae, see e.g., Watson (1998) and Kalajdžić (2010). This allows for reassessment of the mass of displacement which can be calculated as the sum of the weight groups masses. At this stage, the weight groups are not detailed, primarily because the cargo tanks and the related systems and equipment are still undefined. For the sake of brevity these intermediate steps are not shown.

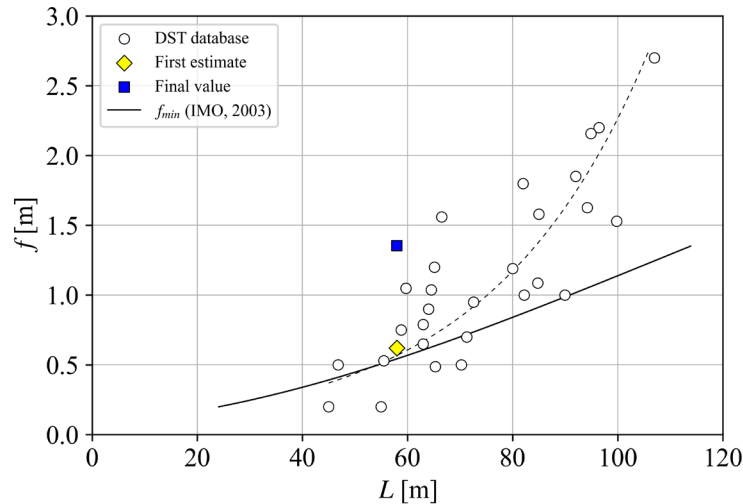


**Figure 4. Comparison of estimated and adopted freeboard to the trend observed in the DST database of relevant ships (dashed line) and to the minimum values required by the International Convention on Load Lines (solid line). Yellow diamond corresponds to the first estimate of the ship freeboard (reported in Table 1). Blue square corresponds to the final value of the ship freeboard (reported in Table 2).**

## HULL FORM AND CARGO TANKS

In absence of the prototype vessel, the initial hull form (see **Figure 5**) was based on typical geometries of coastal cargo ships, as found in e.g., Journee and Versluis (1999). The hull form is subject to modifications which may be needed to accommodate sufficient space for cargo tanks and associated cargo-handling equipment and attain the targeted hull properties (hull form coefficients and the longitudinal center of buoyancy as given in **Table 1**). At this stage, the CAD tools (NAPA Designer and SolidWorks) are extensively used to check the effect of the hull modifications on the sizing and arrangement of the vessel’s main “blocks”: cargo space, machinery rooms, accommodation and working spaces, ballast and fuel tanks, etc.

The shape of cargo tanks intended for liquefied ammonia depends on whether the liquefaction is achieved by pressurizing the gaseous ammonia (resulting in fully pressurized ammonia), by pressurizing in combination with refrigeration (resulting in semi-refrigerated ammonia) or by refrigerating the ammonia to temperatures below  $-33^{\circ}\text{C}$  at ambient pressure (resulting in fully refrigerated ammonia). All the above liquefaction methods are used on seagoing ships, whereby refrigeration is usually used for larger quantities while pressurizing is more often used for the transport of smaller ones. Thus, the decision on the cargo tank geometry and arrangement (which also affects the hull form) depends on the selection of the liquefaction approach. Pressurized and semi-refrigerated ammonia are carried in cylindrical pressure vessels (the so-called Type C tanks). Type C tanks may bring some benefits in view of the simpler (structural) design. On the other hand, the utilization of the hull volume available for cargo space is relatively low with the Type C tanks. Fully refrigerated ammonia is carried in prismatic Type A tanks where overpressure is managed by a boil-off management system, i.e. the re-liquefaction unit. The Type A tanks are self-supporting tanks, typically made of flat surfaces and shaped so as to maximize the space available for cargo. The prismatic tanks may allow up to 40% more cargo containment space (DNV GL, 2019). (For the main features of different types of cargo tanks used on liquefied gas carriers and typical design solutions see e.g. SIGTTO, 2021.) Characteristics of materials suitable for cargo systems of liquefied gas carriers (cargo tanks, process pressure vessels, and cargo piping) are detailed in the International Code for the Construction and Equipment of Ships Carrying Liquefied Gases in Bulk (IGC Code, see IMO, 2014). In view of the small cargo capacity, it was initially assumed that the ammonia would be pressurized and carried in Type C tanks. However, it will be shown that the final decision on the liquefaction method and, consequently, the design of the cargo tanks, depends on several design and operation aspects.

To attain sufficient volume of the cargo space and provide adequate room for the propeller, while maintaining the desired values of the block coefficient and the longitudinal center of buoyancy, it was necessary to increase the depth of the ship, from  $D = 3.87$  m to  $D = 4.77$  m. It was previously indicated that while the increase of freeboard is to the benefit of safety, it

also adds to the production costs (and some operational costs). Nevertheless, as it was pointed out by Schneekluth and Bertram (1998), the depth is the “cheapest” ship dimension since its increase results in a relatively small increase of steel weight. (Interestingly, the new depth value results in  $B/D = 2.2$ , which seems to be the most common ratio for the small gas carriers, see **Figure A1** in the Appendix to the paper.) Additionally, the raising of the deck caused the distortion of the hull lines which led to a decrease of the wetted surface at the stern, which is beneficial from the ship resistance point of view. The evolution of the hull lines of the vessel – from the initial hull form (shown in gray lines) to the final hull form with the raised main deck (shown in blue lines) – is reported in **Figure 5**. The cross sections from “0” to “54” are equally spaced at 1 m distance; the section “-1” is at -1.55 m. In both cases, the sections are shown up to the main deck (i.e., the geometry of the poop and the forecastle is not shown). In addition to attaining the targeted values of  $C_B$  and  $LCB$ , a positive “side effect” of the hull modification is the increase of the waterplane area coefficient in comparison to the first estimate given in **Table 1**, which is beneficial from the seakeeping point of view.

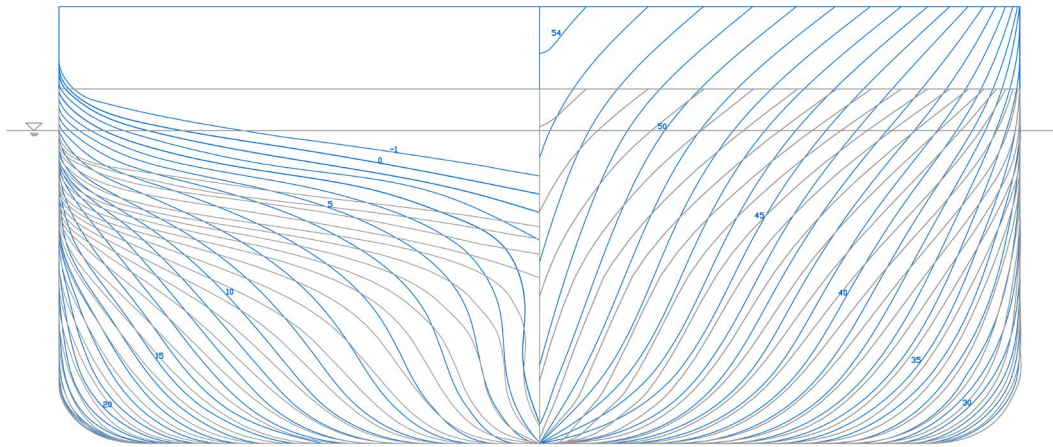


**Figure 5. Body plan of the vessel. The initial hull form is shown in gray lines; final hull form is shown in blue lines.**

The completion of the hull form was followed by the fitting of the cargo tanks. Despite the increase of the ship depth, the Type C tanks intended for pressurized ammonia could not be fitted without further considerable modification of the hull form. In order to comply with the ship survival capability and location of cargo tanks provisions of the 2014 IGC Code, that is, to attain the minimum distances between the cargo tanks and the hull, the diameters of the cylindrical tanks have to be limited. To attain the required cargo volume with the constrained tank diameters, the length of the cylinders has to be increased; this, however, results in the substantial loss of space available for forward and aft engine rooms. A compromise may be partly achieved by positioning the tanks higher relative to the baseline. In such a case, however, intact stability criteria cannot be satisfied. This led to reconsideration of the adopted liquefaction method.

Considering the toxicity of ammonia, a major factor to be accounted for when it comes to the selection of the liquefaction method is safety. As observed by the Society of International Gas Tanker & Terminal Operators, despite a good safety record of gas carriers, the risks related to accidents are greater in ports than at sea (see SIGTTO, 2021). The bunker vessel which is the subject of this study is supposed to serve passenger ferries; the vessel should, thus, operate in the vicinity of the passenger terminals in Travemünde and Rostock where an average of 10 and 20 passenger ships port calls respectively are recorded daily. Therefore, the consequences of potential accidents involving leakage of ammonia may be grave in view of the possibly large number of casualties. The spreading of ammonia in the event of leakage, however, differs depending on the liquefaction method. In the event of refrigerated ammonia leakage, the ammonia gas cloud forms due to evaporation of the cold pool of spilled ammonia (**Figure 6b**). The gas cloud formed as a consequence of pressurized ammonia leakage is significantly larger as it is fed by both a high flow velocity jet from the damaged tank and the evaporation of the pool of spilled ammonia (see **Figure 6a**). Once evaporated ammonia reaches ambient temperature, it will rise – this process will, however, take more time (i.e., the exposure to ammonia will be prolonged) if the ammonia was pressurized.

Some operational aspects may also affect the choice of the liquefaction method. Considering that the vessel should operate in ports and in a coastal area with dense traffic, less obstruction of the view from the wheelhouse could be advantageous. This becomes particularly important in view of complex systems and numerous equipment for handling ammonia and bunkering operations arranged on the main deck. Cylindrical tanks, required for carrying the pressurized ammonia, would have to be positioned higher with respect to the baseline, which could have a negative impact on the visibility from the bridge. Furthermore, in direct relation to the vessel’s purpose – bunkering – it is to be noted that at high pressures required for compression liquefaction the dry disconnect couplings of bunkering hoses cannot be manually operated by the crew.

Therefore, based on the considerations given above (space utilization, safety, and operational aspects) it was decided to change the liquefaction method used on the bunker vessel. Instead of carrying pressurized ammonia in the cylindrical Type C tanks (Figure 7a), the vessel would carry refrigerated ammonia in the prismatic Type A tanks (Figure 7b) which would be a common solution on large liquefied gas carriers, rather than on small ones (see SIGTTO, 2021). The space utilization with Type A tanks would be indeed much better: the total length of the Type A tanks is 26.5 m, while the length of the Type C tanks would be (at least) 33.4 m. The visibility from the bridge would also improve: the highest point on the tank covers relative to the baseline would be 6.68 m for Type A tanks, as compared to (at least) 8.1 m for Type C tanks. The stability and survivability requirements can be satisfied in all relevant loading conditions if Type A tanks are utilized.

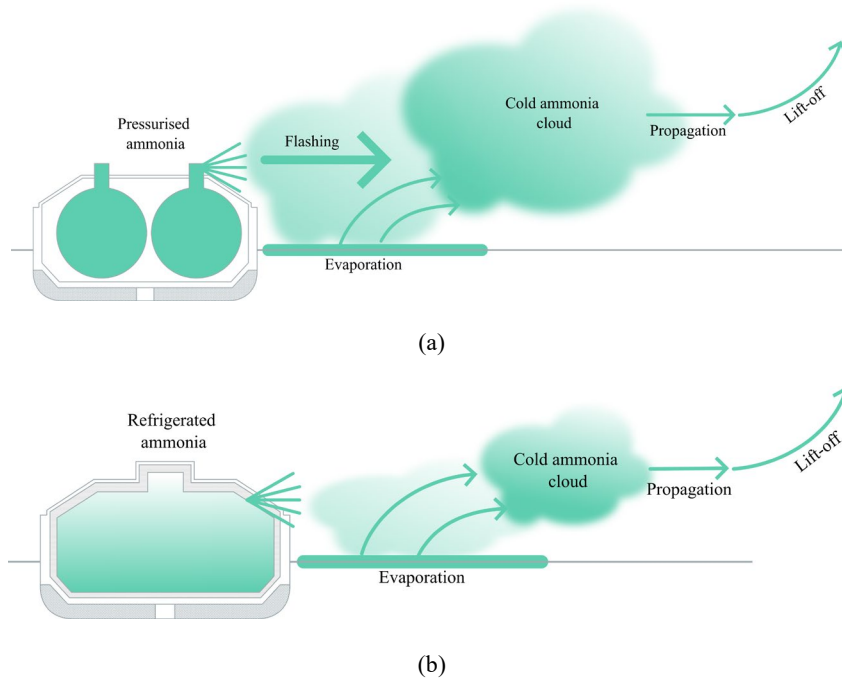


Figure 6. Spreading of ammonia in case of leakage of (a) pressurized ammonia and (b) refrigerated ammonia.

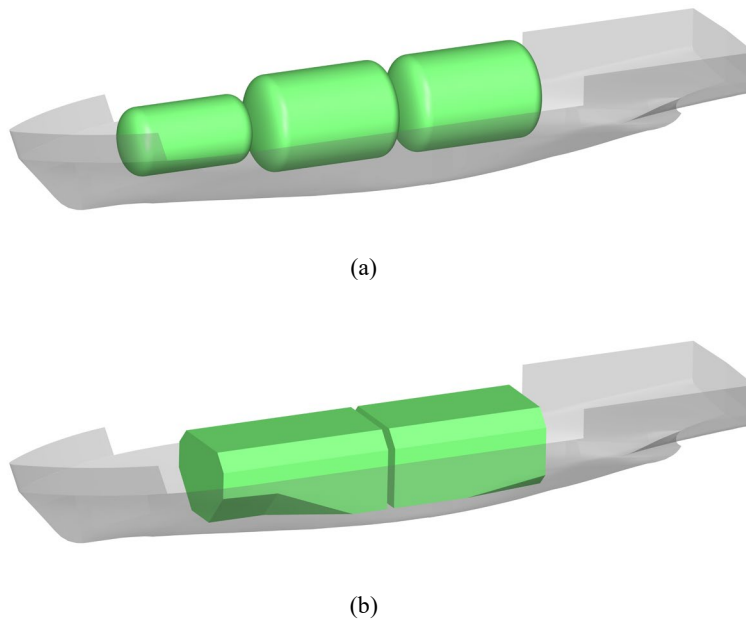


Figure 7. Comparison of the space requirements for (a) pressurized ammonia carried in the Type C tanks and (b) refrigerated ammonia carried in the Type A tanks.

This allows for a more precise estimation of weight groups' masses and centroids. The mass of the cargo tanks, which form a sizable part of the lightship mass and thus can significantly affect a range of design aspects, can be assessed based on the detailed CAD model of the tanks built in SolidWorks. The specific equipment and systems used for handling of ammonia could be itemized. Other weight groups may be determined with more reliability as well. The mass of machinery may be based on the actual main engine; the corresponding fuel consumption allows us to determine the required fuel supplies more precisely. The actual dimensions of the accommodations, poop and forecastle may be used in steel weight estimation, etc. The knowledge of the weight groups' masses and centroids makes it possible to determine the floating position of the ship in a range of relevant loading conditions and to calculate the ship stability parameters and compare them to the applicable regulatory requirements.

The main ship particulars, as adopted, are given in **Table 2**. The final value of the mass of displacement is less than 5% greater than the initially estimated value reported in **Table 1** (despite the increase of the depth), which is generally regarded to be within the acceptable boundaries. Greater differences would indicate that the main dimensions were not properly selected, which would require the process to be restarted, instead of advancing to the next stage of design. Considering the large initial uncertainty related to the type and size of cargo tanks and the related equipment, the questionable adequacy of formulae used in early stages, as well as the lack of an adequate prototype vessel which would be normally used in the estimation of the weight groups, the relatively low deviation of the mass of displacement from the preliminary assessment is most certainly a positive, yet (admittedly) somewhat unexpected outcome.

**Table 2. Main ship particulars**

Cargo capacity	$V_{cargo}$	1000 m <sup>3</sup>
Mass of deadweight	$m_{DWT}$	746.4 t
Displacement	$\Delta$	1337.8 t
Length over all	$LOA$	58 m
Length between perpendiculars	$L_{pp}$	56.869 m
Beam	$B$	10.5 m
Draught	$d$	3.415 m
Depth	$D$	4.77 m
Freeboard	$f$	1.355 m
Block coefficient	$C_B$	0.624
Waterplane area coefficient	$C_{WL}$	0.833
Midship area coefficient	$C_M$	0.992
Longitudinal center of buoyancy	$LCB^*$	-2.1 %L

\* In reference to midships

## DECK ARRANGEMENT

One of the design objectives is safe and efficient handling of ammonia in the course of loading and bunkering operations. This requires the vessel to be outfitted with specific systems and equipment, which ought to be adequately arranged on the main deck. To facilitate a fitting positioning of the installations for handling of the ammonia, the 3D model of the ship built in SolidWorks was utilized, see **Figure 8**. The systems include manifolds (position 1 in **Figure 8**) to connect the bunker line (represented in green), the purge line (represented in light blue) and the vapor return line (represented in yellow) suitably positioned along the parallel midship. A vapor return line is necessary as during bunkering no gaseous ammonia in the customer's bunker tank may be vented to the open air; to avoid the pressure build-up, the gaseous ammonia shall be taken over by the bunker vessel. Via the purge line all lines can be purged with nitrogen. Via the condensate return line the reliquefied boil-off gas can be given back from the re-liquefaction unit in the forecastle to the cargo tanks. In case of an emergency such as tank over-pressure, both tanks are equipped with redundant pressure relief valves. The emerging ammonia is then led to the vent mast (position 2 in **Figure 8**). The IGC Code states that cargo tank venting openings "shall be arranged at distance at least equal to  $B$  or 25 m, whichever is less, from the nearest air intake, outlet or opening to accommodation spaces, service spaces and control stations, other non-hazardous areas, exhaust outlet from machinery or from furnace installations onboard" (IMO, 2014). Since the area around the manifold is regarded as a work area, the vent mast is placed furthest away.

In addition to the manifold, the vessel is equipped with a bunker arm (position 3 in **Figure 8**) to serve customers with a high freeboard. A set of all bunker lines is directly attached to the arm. Bunker hoses can be stored on deck. To keep a safe distance from customers, the bunker vessel has four Yokohama fenders (position 4 in **Figure 8**). The safe distance also ensures that the bunker hose is not pinched or kinked during the bunker process.

All the auxiliary equipment, such as the re-liquefaction unit and the nitrogen plant, is stored in the forecastle, away from the bunker area. Often, on board larger ships, there is a dedicated deck house in the midship area. For this design it is assumed that the vessel is mainly operated very close to the shore/the terminal and does not need the amount of inert gas that a large gas carrier would need. Also, the re-liquefaction unit is rather small, and the ammonia is only transported over a relatively short distance to the next customer.

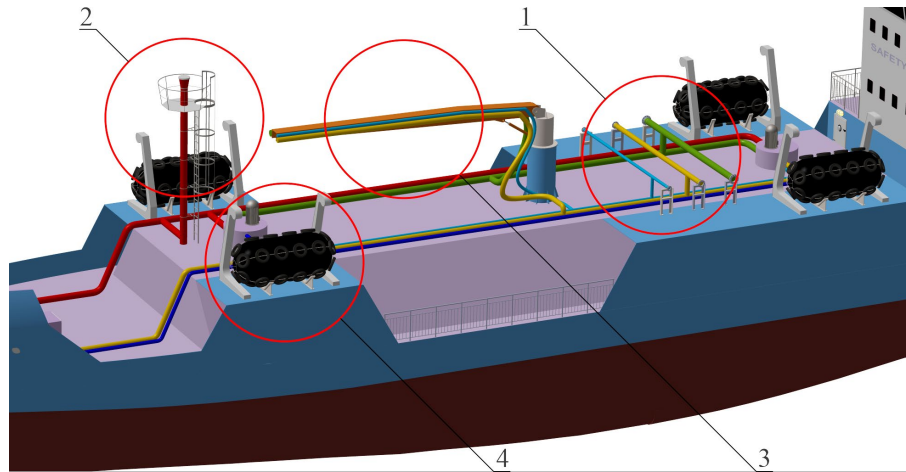


**Figure 8. Simplified view of the main deck: arrangement of systems and equipment for handling of the ammonia**

## POWER PREDICTION AND MODEL TESTS

Ship resistance and power demand were estimated in each of the described design phases. The resistance estimations were carried out using the well-known empiric methods, such as the “Holtrop & Mennen” (see Holtrop, 1984) and the “Admiralty coefficient” approach (see Telfer, 1963) which is based on the data of comparable ships. Additionally, the resistance and propulsion model tests with a 1:14.5 scale model were performed in the large shallow water basin of DST, at two different water depths corresponding to  $h_w = 12.5$  m and  $h_w = 5$  m in full scale. Effective power calculated based on the resistance estimations made by the empiric methods and the model tests are reported in **Figure 9**.

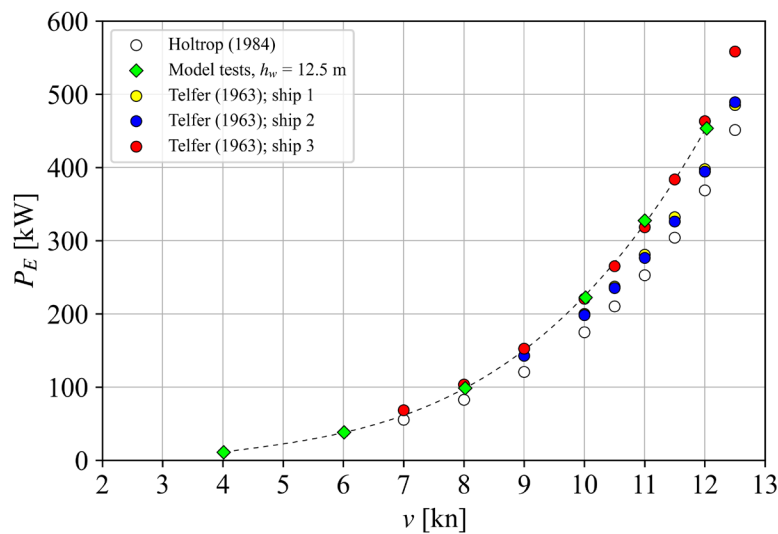


**Figure 9. Comparison of effective power calculated using resistance estimations obtained with empiric methods and by means of model tests performed in the towing tank of DST.**

The ship has a conventional drivetrain consisting of a diesel engine (691 kW@1406 rpm). The model was equipped with a four-bladed DST stock propeller (the propeller diameter being  $D_p = 1.84$  m in full scale, and pitch ratio being  $P/D_p = 0.955$ ). Since the main engine was selected based on the estimations done with empiric methods in the course of the basic design, the model tests were primarily used to verify if the predicted power would satisfy the owner's requirements. In addition, the model tests allow us to assess the reliability of the aforementioned empiric methods which are often used in the basic design. For instance, it may be observed that the Holtrop & Mennen method underestimates the resistance obtained in the model tests by some 20%. On the other hand, the best prediction was achieved using the Admiralty coefficient approach based on "ship 3" (red circles in **Figure 9**), which is indeed the most comparable one to the designed vessel (see **Table 3**).

**Table 3. Features of the ships used in the ship resistance estimation based on the Admiralty coefficient approach.**

	"ship 1"	"ship 2"	"ship 3"	design
$L_{pp}$ [m]	63.4	48	66	56.869
$L / \sqrt[3]{\nabla}$ [-]	5.62	4.71	4.95	5.21
$B/d$ [-]	3.58	3.53	3.41	3.07

Finally, the comparison of the total resistance recorded in model tests performed in two selected depths is reported in **Figure 10**. The chosen water depths are representative of the operational conditions in the designated area. As expected, a significant increase in resistance and, consequently, a reduction of speed in  $h_w = 5$  m can be observed, which needs to be considered in the prediction of the operational profiles.

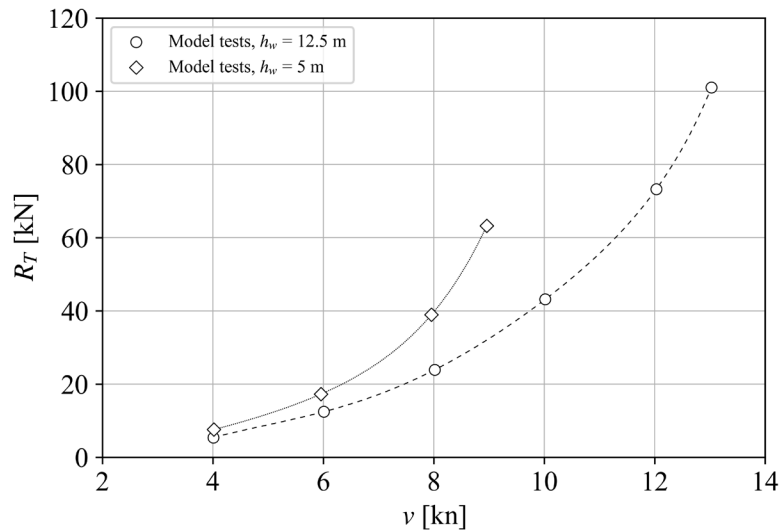


**Figure 10. Comparison of total resistance obtained in model tests performed in the towing tank of DST in both tested water depths.**

## CONCLUSIONS

Energy transition of shipping goes beyond the modification of the ship propulsion and fuel systems and requires the development of the supporting infrastructure, including the vessels which could provide the bunkering service to ships utilizing novel fuels. The paper presented the basic design of a small ammonia bunker vessel, intended to provide ship-to-ship refueling services to future ammonia-powered ferries in the South Baltic Sea. Because of the size of the vessel (dictated by the cargo capacity at the lower boundary of capacities of the present ships) and its specific purpose (bunkering of passenger ships with toxic ammonia), the existing gas carriers could not be successfully used as prototypes. However, the formulae typically used in early stages of design (which may be found in the literature) proved to be robust enough to predict the vessel's mass of displacement and the main particulars with sufficient accuracy, despite not being developed with this specific ship type in mind. The inability to utilize the ship design spiral in a straightforward manner due to the absence of the prototype vessels was compensated for with an extensive use of CAD tools (NAPA Designer and SolidWorks) which facilitated architectural design of the vessel (i.e., arrangement of spaces and equipment) and minimized the uncertainties related to weight estimations.

The design is heavily influenced by the liquefaction method of ammonia, which in turn, depends on the ship operational profile and safety requirements. Even though liquefaction by pressurizing is typically used in maritime transport of smaller quantities of ammonia, in this case, the adopted liquefaction method was full refrigeration. Such a decision was driven by several design and operational aspects including much better cargo space utilization than it would be achieved by the pressurizing of ammonia, compliance with the survivability requirements of the IGC Code and intact stability requirements of the IS Code, more favorable dynamics of spreading of the toxic ammonia cloud in case of a spillage, and better visibility from the bridge (see Yang et al., 2022; SIGTTO, 2021; DNV, 2020; DNV GL, 2019). Again, the CAD tools enabled the sizing and positioning of the cargo tanks and arrangement of the associated systems and equipment, and fast verification of compliance with the design objectives and applicable regulations.

It is to be acknowledged that, considering the scarcity of adequate data which could be used in support of the decision-making, as well as the nonexistence of the design guidelines specifically intended for this kind of bunker ships, many decisions had to be made by the “designer” with the support of the CAD tools. This indicates that the design process could be further improved by implementing an automated multi-objective optimization (a “holistic ship design” as described in e.g., Papanikolaou, 2010; Marzi et al., 2018) provided that adequate software tools and computing resources are available. Such an approach allows for a fast analysis of dependencies between influential factors and exploration of a large number of (feasible) designs in search of an optimal solution. Nevertheless, regardless of accessibility of the tools and the implemented procedure, it is the designer who formulates the optimization criteria by considering the relevant regulatory, societal, and commercial aspects. In case of ammonia bunker vessel analyzed in this study, the formulation of criteria requires the knowledge of intricacies of energy transition, the understanding of operational risks associated with bunkering of ammonia, the specific environmental conditions in the operational area, etc.

The outcome of the study – presented in **Figure 11** – is a design which may be regarded as unconventional, primarily due to a fine hull form atypical for bunker ships and the adopted type of cargo tanks which is not common for small liquefied gas carriers. The success of the design was partly assessed with the model tests described in this paper, which addressed powering requirements in calm water. The design will be, however, the subject of the extended model tests which shall include the seakeeping performance and stability in waves of the vessel with partially filled cargo tanks. Only then, the success of the proposed design may be fully appreciated. Nevertheless, the outcome of the study indicates that the energy transition may require the development of new designs rather than reiteration of “off-the-shelf” ship design solutions.

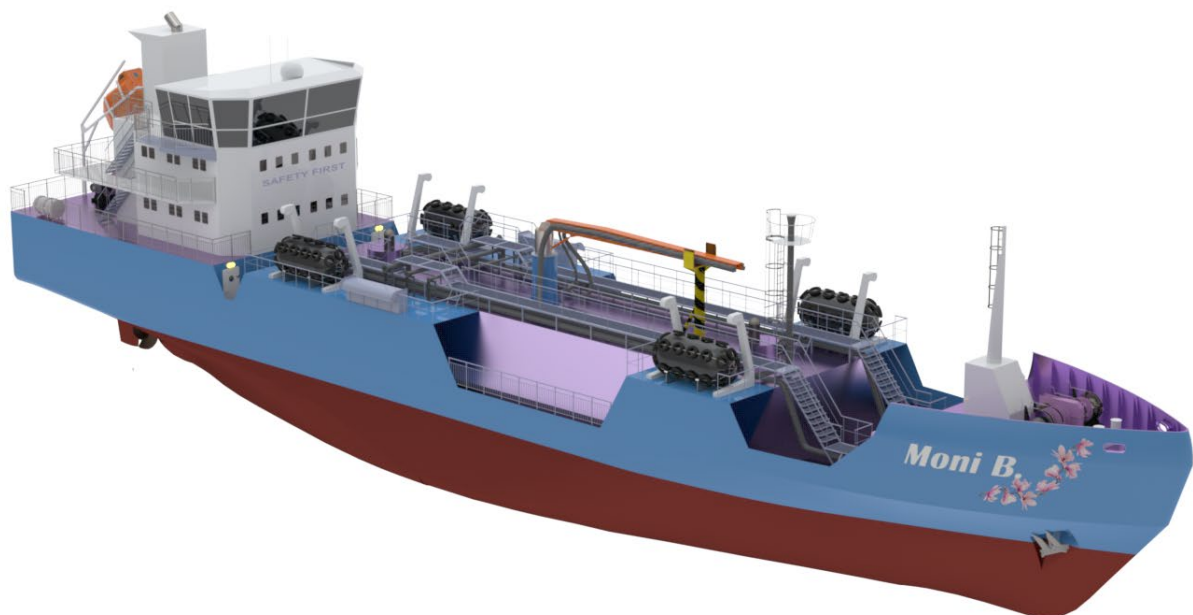


**Figure 11. Final layout of the coastal ammonia bunker vessel**

## CONTRIBUTION STATEMENT

Friederike Dahlke-Wallat: Formal analysis, investigation, visualization, writing – original draft, writing – review & editing. Katja Hoyer: Formal analysis. Ljubisav Isidorović: Visualization. Sophie Martens: Formal analysis, investigation, writing – review & editing. Nathalie Reinach: Formal analysis, visualization. Benjamin Friedhoff: Funding acquisition, project administration, resources, supervision, writing – review & editing. Igor Bačkalov: Conceptualization, formal analysis, investigation, methodology, visualization, writing – original draft, writing – review & editing.

## ACKNOWLEDGEMENTS

The research presented in this paper was funded by the German Federal Ministry of Education and Research (BMBF) within the framework of the hydrogen flagship project TransHyDE within the CAMPFIRE sub-project “Flexible NH<sub>3</sub>-refueling system” (No. 03HY209D).

## REFERENCES

- Barras, C.B. (2006). *Ship Design and Performance for Masters and Mates*. Second Edition. Oxford: Elsevier Butterworth-Heinemann.
- DNV (2020). *Ammonia as a marine fuel safety handbook*. Retrieved from <https://www.dnv.com/Publications/ammonia-as-a-marine-fuel-191385>.
- DNV GL (2019). *LNG containment systems: Finding the way for Type A*. Retrieved from <https://www.dnv.com/expert-story/maritime-impact/LNG-containment-systems-finding-the-way-for-Type-A/>.
- Holtrop, J. (1984). *A statistical re-analysis of resistance and propulsion data*. International Shipbuilding Progress, 31(363), 272–276.
- IMO (2003). *International Convention on Load Lines*. London: International Maritime Organization.
- IMO (2014). *International Code for the Construction and Equipment of Ships Carrying Liquefied Gases in Bulk (2014 IGC Code)*. London: International Maritime Organization.
- Journee, J.M.J. and Versluis, A. (1999). *Hull Form Series for SEAWAY*. Report No. 1206-M. Delft: Delft University of Technology, Faculty of Marine Technology, Ship Hydromechanics Laboratory.
- Kalajdžić, I. (2010). *Cargo ships weight groups calculation*. Master thesis. Belgrade: University of Belgrade, Faculty of Mechanical Engineering.
- Marzi, J., Papanikolaou, A., Brunswig, J., Corrigan, P., Lecointre, L., Aubert, A., Zaraphonitis, G., Harries, S. (2018). *HOLISTIC ship design optimisation*. Proceedings of the 13<sup>th</sup> International Marine Design Conference. Helsinki.
- Papanikolaou, A. (2010). *Holistic ship design optimization*. Computer-Aided Design, 42(11), 1028–1044.
- Papanikolaou, A. (2014). *Ship Design: Methodologies of Preliminary Design*. Dordrecht Heidelberg New York London: Springer.
- Schneekluth, H. and Bertram, V. (1998). *Ship Design for Efficiency and Economy*. Second Edition. Oxford: Butterworth-Heinemann.
- SIGTTO (2021). *Liquefied Gas Handling Principles on Ships and in Terminals*. Livingston: Witherby Publishing Group Ltd.
- Takahashi, H., Goto, A., Abe, M. (2006). *Study on Standards for Main Dimensions of the Design Ship*. Technical note of National Institute for Land and Infrastructure Management. Tokyo: Ministry of Land, Infrastructure and Transport.
- Watson, D.G.M. (1998). *Practical ship design*. Oxford: Elsevier Science Ltd.
- Yang, M., Ng, C.K.L., Liu, M. (2022). *Ammonia as a marine fuel - bunkering, safety and release simulations*. Singapore: Singapore Maritime Institute.

# APPENDIX

Features of the DST database of the relevant ships used in verification of the selected main particulars.

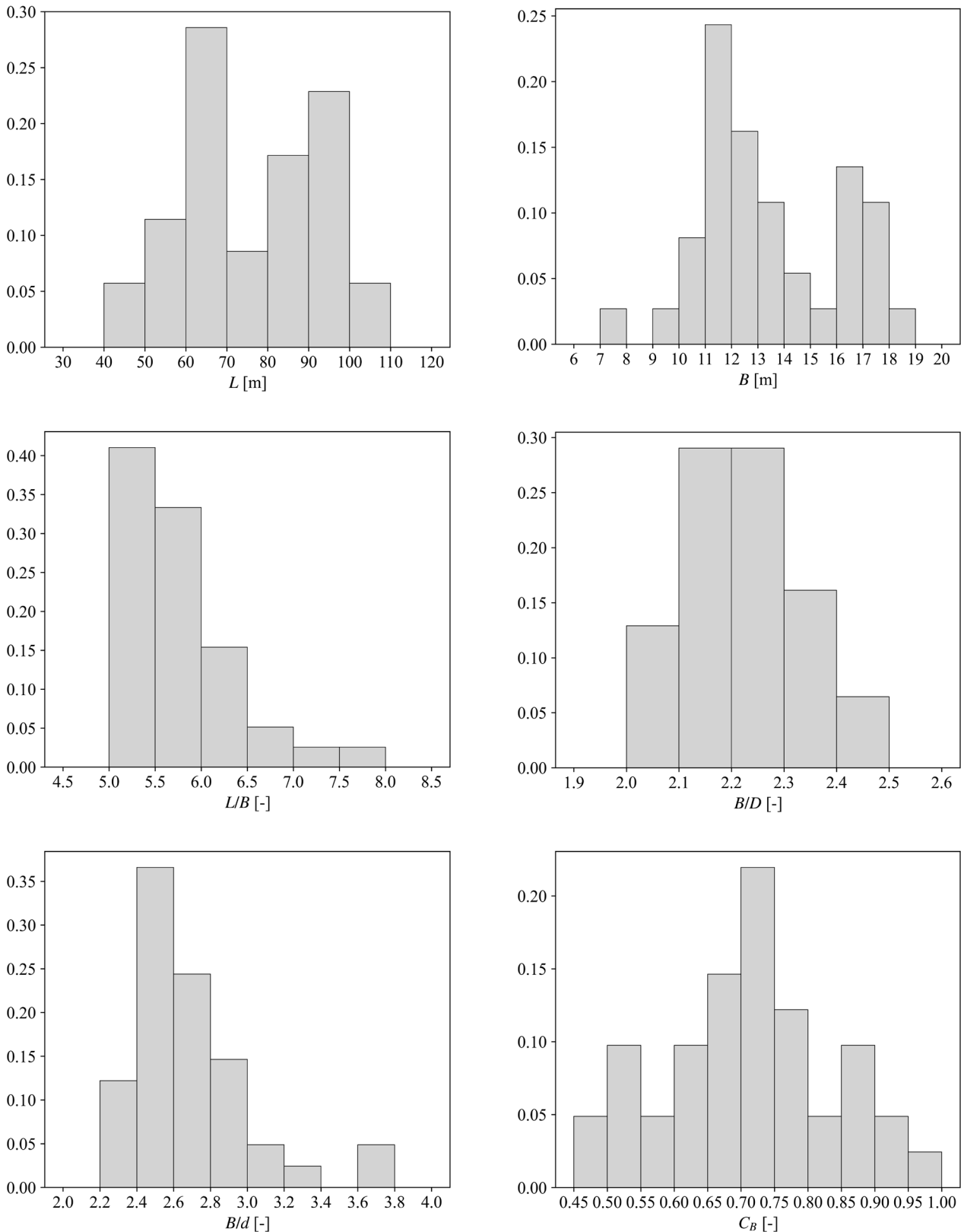


**Figure A1.** Distributions of the main dimensions, ratios, and hull form coefficients of the ships contained in the DST database of relevant ships.